April 1999 ECN-R--99-001

VOLATILE ORGANIC COMPOUNDS AND AEROSOLS IN AIR

Development of sampling methods, chemical analysis and modelling

Alex Vermeulen
Frits Bakker
Marco Geusebroek
Andrey Khlystov
Jan Willem Erisman

Revisions		
A		
B		
Made by: A.T. Vermeulen 8-06-00	Approved by: J. Slanina	ECN-Fuels, Conversion & Environment Air Quality
Checked by: A. Hensen 26-5-99	Issued by: C.A.M. v.d. Klein	

Abstract

Emissions of traffic contribute to a large extent to the health effects of air pollution. It is still uncertain how much of these effects are due to aerosols and whether chemical composition or just the number of particles are important. The interactions between gaseous and particulate matter in the atmosphere requires that scientific studies will have to deal with those interdependencies. Computer models will be very useful here, but these models must be evaluated using measurements. Good and useful measurements to test these models are scarce.
Sampling and analysis of organic compounds in gaseous and particulate phase in the atmosphere is a complex job. To study the relative importance of the possible processes in the atmosphere in the first half hour after emission of organic compounds, measurements and computer models to test (the gaps in) our knowledge are required. In this report the analytical and sampling methods deployed or developed to do this are described. During an experiment along the A9 highway the sampling and analysis techniques were tested. Within certain limitations all methods deployed are adequate for use in further research.
Modelling tools are developed and adopted to describe the dispersion process, chemical reactions, deposition and aerosol processes.

Keywords
VOC, PAH, aerosol, aerosol size distribution, photochemistry, dispersion modelling, atmospheric chemistry, concentration measurement, aerosol sampling, ozone, vehicle emissions.

Acknowledgement/Preface

This report is a result of the research project with ECN number 7.2693 and the air research part of a project funded by the Ministry of Transport under ECN number 7.2696.01.06.
The STEM III code was kindly provided by Prof. G. Carmichael of the University of Iowa.

CONTENTS

SAMENVATTING

Emissies van verkeer en vervoer dragen voor een aanzienlijk deel bij aan de gezondheidseffecten van luchtverontreiniging. Onbekend is nog hoe groot de rol van deeltjes (aërosolen) in die effecten is en of dat samenhangt met de chemische samenstelling of puur met het aantal deeltjes. De interactie tussen gasvormige luchtverontreiniging en bijvoorbeeld fotochemie van de atmosfeer en de dynamiek van deeltjesvorming betekent dat deze zaken in onderling verband bestudeerd moeten worden. Modellen zijn daarbij onmisbaar. Die modellen moeten echter getoetst worden aan metingen. Goede en bruikbare metingen zijn schaars.
Monstername en analyse van organische stoffen in de gas- en deeltjesfase in de atmosfeer is een complex proces. Doel van het onderzoek in dit rapport is het ontwikkelen en testen van gedeeltelijk reeds aanwezige en verder te ontwikkelen methoden op het gebied van meting en modellering van die organische verbindingen in de atmosfeer. Gedurende een experiment langs de snelweg A9 zijn de monstername- en analysetechnieken getest. Binnen zekere beperkingen zijn de gebruikte methoden uitstekend geschikt voor gebruik binnen verder onderzoek.
Modelleer gereedschappen zijn verkregen en verder ontwikkeld om de processen van belang in de atmosfeer (te weten dispersie, chemische reacties, depositie en aerosol processen) te beschrijven.

1. INTRODUCTION

Emissions of traffic contribute to a large extent to the health effects of air pollution. It is still uncertain how much of these effects are due to aerosols and whether chemical composition or just the number of particles are important (Peters et al., 1997).
Large quantities of volatile and semi-volatile organic compounds (VOC, SOC) are emitted into the atmosphere because of both natural and anthropogenic activities. These compounds then will interact through complex mechanisms with other chemical compounds in the atmosphere, a process in which UV radiation from sunlight plays an important role. This will result in effects like for example photochemical air pollution, changes in stratospheric ozone and acid deposition.
A complicating factor in the complex path of emission-degradation-deposition is the gas-particulate phase partitioning in the atmosphere of the organic substances, as this affects to a large extent the residence times. Rapid changes in the gas-particulate phase partitioning occur in the first minutes after emission from most sources. A large amount of organic matter of anthropogenic origin is released through combustion processes. In the first moments after emission due to combustion large changes in temperature, relative humidity and other important factors occur, giving rise to tremendous changes in the distribution of organic compounds between the gaseous and the particulate phase.
Usually the emissions are measured right before or after emission into the atmosphere. These emission rates are then used in dispersion models of different scales (from local to global) to predict imission (concentration levels). The emission rates used in those dispersion models however have different time and spatial scales as the emission rate measurements. A translation is needed from the emission rate as measured directly at the source to the emission rate on the scales that are used by the different models, accounting for the processes that will take place on the intermediate level.
The gas-particulate phase partitioning also complicates the sampling process for concentration measurements (for emission rate determination or imission measurements). Usually filter-absorbent methods are used that are known to show artefacts like losses from the gas trap, absorption of gases on trapped particles, transmission of very small particles, degradation of chemicals during the sampling procedure and desorption of gases from the filter-bound substances (Kaupp & Umlauf, 1992). The analysis of very small amounts of organic material, analysed with HPLC or GC-MS methods for a large number of components is a major challenge.
The research at ECN Environmental Quality & Technology is and has been targeted at several of the subjects mentioned in the text above. Throughout the years large experience has been built up with sampling of particulate matter and determining size distribution and chemical composition. For the gaseous phase, the emphasis has until now been on measuring and modelling of the behaviour of the inorganic species, like SO_2 and NH_3, in the atmosphere. Starting 1994, an EC project has been carried out to study the ratio of anthropogenic and biogenic emissions of VOC's through the analysis of isotopic ratios (Slanina et al, 1998).
The main objective of the project described in this report is to build the expertise in sampling and analysing of VOC's in gas and particulate phase in air, in order to be able to measure the relation between direct emissions and the emission fields that need to be resolved for use in local, regional, continental and global scale models.
Also this project has been used to acquire and develop the model parts that are needed to describe, study and understand the fate of VOC's and aerosols in about the first 30 minutes after release into the atmosphere. This will enable to couple measurements performed at some distance from sources with models to derive the parametrisations needed to drive larger scale models with the correct emissions of VOC's and aerosol size distribution and composition.

In the current air pollution models the gas-particulate phase partitioning is not treated at all or in a highly simplified manner. Recently the attention for this important subject has increased. Lack of measurements however prevent the validation of these modelling efforts.
Thorough model analysis of the processes in the particulate phase also requires substantial computing resources. Current state of the art Eulerian regional transport models containing atmospheric photochemistry require already so much computing power that even on supercomputers the calculations run in about real-time or only slightly faster. Inclusion of the state of the art description of the particulate phase slowed down the calculations with a factor of 20 (Carmichael, pers. comm.). Despite the fast developments in computer hardware it will take some time before such an increase in needed computing resources can be justified. One of the targets of the research is to increase our understanding of and to select those processes that need to be described to significantly enhance the computer models, depending on their scale and application.
The experiments were targeted at one of the largest antropogenic source of aerosols and VOC's, i.e. road transport.
In this report first the applied techniques for sampling and chemical analysis will be described. In the next chapter the model selection and developments are described, followed by a chapter on the road experiment and the results of the measurements. In the last chapter the results of the project are discussed and the perspective for future work on the topic is given.

2. SAMPLING AND ANALYSIS TECHNIQUES

2.1 General

The description of each of the techniques referred to in this chapter could fill one or more books on its own. But as most techniques are based on current standards for air pollution monitoring only short descriptions of the techniques and materials developed or used for the first time in our laboratory for this project will be given.

2.2 PUF/filter aerosol+gas sampling

The poly-urethane foam/filter combinations are built and used according to the ISO/DIS 12884 standard. ECN produced for this project the aluminium PUF/Filter holders needed to sample air at flows between 100 and 250 $l.min^{-1}$ (maximum volume sampled is 350 m^3).
Before usage the PUF plugs are cleaned by ultrasonic extraction with acetone for 1 hour, followed by 3 hours of drying at 40°C and ultrasonic extraction with toluene for 1 hour, followed again by 3 hours of drying at 40°C. After sampling the filters are extracted with 100 ml of toluene, the PUF samples are extracted with 200 ml of toluene, all for a period of 1 hour in an ultrasonic bath in 500 ml bottles, the toluene is then brought into 250 ml glass beakers, the toluene remaining on the filters resp. plugs is weighed and corrected for, assuming a homogeneous distribution of all material over the toluene in the plug and in the beaker. The next step is concentration by evaporation of the toluene at 100 °C to a volume of 2 ml. The sample solution is then brought into 15 ml Kuderna-Danish tubes. The glass beakers are rinsed three times with 1 ml of toluene that is then added to the sample liquid in the KD tubes. This solution is again concentrated by evaporation under a N_2 flow to a minimum volume and brought into a weighed crimp-vial. The KD tubes are rinsed twice with 0.4 ml of acetonitril, which is added to the crimp-vial. The vial is then weighed back to determine the sample weight. The efficiency of the analytical process is tested by adding a known amount of EPA-12 PAH standard to PUF and filter material followed by the extraction procedure described above. The recoveries have acceptable values that range from 70-90%. Acceptable values according to the ISO/DIS standard are 50-150%.

2.3 Impactor aerosol sampling

Aerosol size distribution and the sampling for chemical composition of the different size classes can be performed by using Sierra cascade impactors. At a flow of 1 m^3 per minute air is drawn through this impactor, on which aerosol is impacted on five paper ‘slotted’ filters and one backup filter. So the aerosols are divided by the Sierra cascade impactors in six size classes as follows:

- 7.2-∞ µm
- 3-7.2 µm
- 1.5-3 µm
- 0.95-1.5 µm
- 0.49-0.95 µm
- 0-0.49 µm (backup filter)

Before and after sampling the filters are conditioned at a certain temperature and relative humidity and weighed to determine the total aerosol mass collected on the filter material (Whatman-41). After sampling the filters are cut into pieces before extraction for the different

chemical analysis techniques to be applied. The filters were analysed in this project on EPA-16 PAH, heavy metals and ^{14}C benzo[a]pyrene. The ^{14}C analysis is discussed in paragraph 2.10.
As a reference for the size distribution Berner cascade impactors are available that allow for the measurement of aerosol mass for shorter intervals and higher precision because of the lower weight and better conditionality of the impaction material (aluminium foil).

2.4 SJAC aerosol sampling

The SJAC aerosol measurement system is a development of ECN. The sampled air is saturated with water vapour by adding a steam-jet to the sample flow in a mixing room, the aerosols in the sample air therefore form water droplets that are separated from the air in a cyclone. The resulting liquid with the dissolved aerosols is then analysed online on a liquid ion chromatograph or stored using a sample changer for off-line analysis. Figure 2.1 illustrates the working principle of the SJAC. It has originally been developed by ECN for sampling of ammoniumsulphate and ammoniumnitrate aerosols, then the SJAC is combined with a rotating wet annular denuder to also sample and separate first the gaseous ammonia and nitric acid (Khystov et al., 1995). But the SJAC can also be used to sample other particulate matter.

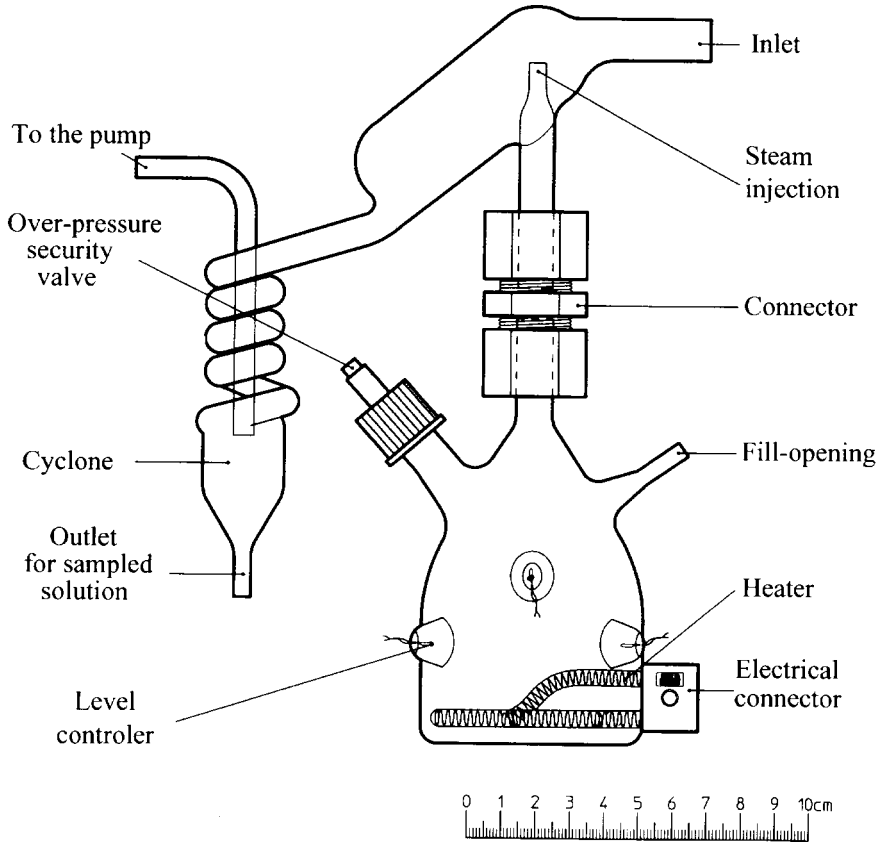

Figure 2.1 Schematic drawing of the SJAC aerosol collector

2.5 Charcoal gas sampling

Charcoal tubes are used to sample C_5-C_9 hydrocarbons. The 'coconut' charcoal tubes deployed are manufactured by Supelco (type ORBO). Sampling of air takes place by pumping an airflow of 500 ml.min^{-1} (controlled through a critical capillary) through the tubes using a 9 Volt battery operated electric mini pump for several hours. After sampling the charcoal tubes are sealed and extracted in the laboratory with CS_2, followed by quantitative transfer into acetonitril. The resulting solution can be analysed directly using GC-MS or HPLC. The sample flows were checked before and after each sample period using a Gill flowmeter.

2.6 Sample bag gas sampling

The filling of the 10 l teflon coated polyethylene sampling bags is performed by pumping ambient air with a flow of about 50 ml.min^{-1} through a 9 Volt battery operated electric micro pump for several hours. The flow is controlled by a critical orifice. The sample flow was measured before and after each sample period using a Gill flowmeter. After sampling the bags were transported to the lab and the next day the sampled air was led into an evacuated glass bulb of 1 liter. The air in the bulb was then preconcentrated using a liquid nitrogen trap. By slowly heating of the trapped sample material the material we are interested in is separated from the relatively volatile O_2, N_2 and CO_2 in the sample air and led into the GC-MS system for further analysis. Sample bags can be used to sample C_2-C_5 hydrocarbons.

2.7 AAS/ICP analysis

Analysis of heavy metals is performed by graphite oven AAS with Zeeman correction. Arsenic is analysed by hydride AAS. The filter material is extracted using nitric acid.

2.8 HPLC analysis

The HPLC system is a HP1100 system, using an acetonitril/water mix as eluens at a flow of 1 ml/min, a Supelcosil LC-PAH column, and the injection volume is 10 µl. The detectors are a FLD, emitting at 350 nm and excitation at 224 nm, and a diode array UV detector at 254.4 nm. The system is run using the HP Chemstation for LC software. Calibration for the PAH's is performed by using the EPA-13 and EPA-16 standard. A typical chromatogram is shown in Fig. 2.2.

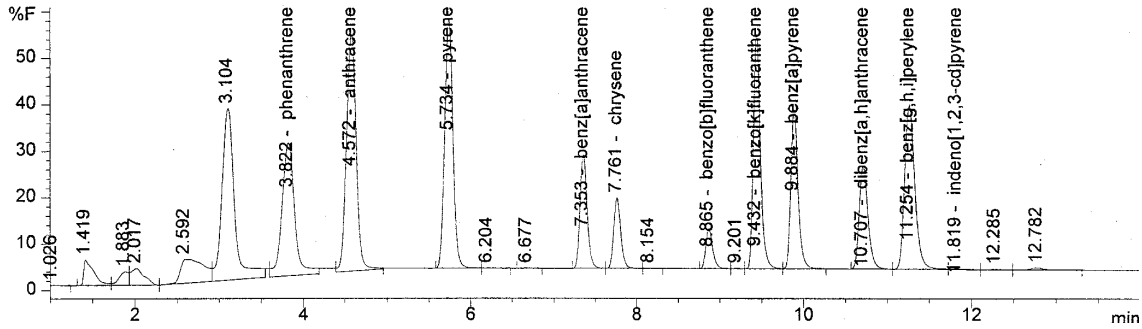

Figure 2.2 HPLC chromatogram of the FLD detector for a HVS air sample.

2.9 GC-MS analysis

The GC-MS system consists of a Carlo Erba GC8060 system equipped with a PORAPLOT QHT capillairy column and a Carlo Erba El980 FID detector. The MS system consists of a Carlo Erba MD800. The systems are driven by two PC's running Interscience ChromCard and Masslab software respectively. A photograph of the GC-MS setup is displayed in fig 2.3.

Figure 2.3 GC-MS system at the ECN laboratory

2.10 ^{14}C measurements

To test the sampling artifacts of the PUF/filter combination and the Sierra impactor backup filter 10 µl of solution contaning ^{14}C enriched benzo[a]pyrene (1.9 MDPM/ml) was added to one half of the filter material before sampling. After sampling the filters were divided in two parts and the part containing the ^{14}C spiked material was analysed for ^{14}C activity using a scintillometer. When part of the benzo[a]pyrene is evaporated from the filter a lower ^{14}C amount will be found. Also chemical reactions of the benzo[a]pyrene can lead to the formation of more volatile products and a lower ^{14}C content on the filter material.

2.11 Aerosol size distribution measurements

To measure the number of particle per class of a certain size, different measurement techniques are available at ECN. The number of particles between 10 nm and 10 µm can be measured using a Condensation Particle Counter (CPC). By combination of the CPC with the SMPS instrument this number can be measured as a function of aerosol size in the range from 5-500 nm. The LAS-X instrument enables to measure the number of particles per size class in the size range from 300 nm-10 µm.

3. ATMOSPHERIC MODELLING OF DISPERSION AND DYNAMIC BEHAVIOUR OF VOCS AND AEROSOLS

In this chapter the models and usuable model parts available at ECN, the models examined for usability of their parts in the project and the models developed during this project are described and discussed.

3.1 Dispersion module (K-model)

The central formulation in K-models for describing the processes in the atmosphere after emission is the following differential equation:

$$\frac{\partial C}{\partial t} = \frac{\partial}{\partial x}\left(K_x \frac{\partial C}{\partial x}\right) + \frac{\partial}{\partial y}\left(K_y \frac{\partial C}{\partial y}\right) + \frac{\partial}{\partial z}\left(K_z \frac{\partial C}{\partial z}\right) - u\frac{\partial C}{\partial x} - v\frac{\partial C}{\partial y} - w\frac{\partial C}{\partial z} + \frac{Q}{\partial x \partial y \partial z} - kC - v_c C \qquad \{1\}$$

which lists in this order the turbulent diffusion, the transport, the source, the chemical conversion and the deposition terms. Solving this equation requires substantial amount of computing resources and adaptation to the scales and conditions of the application, so for daily use, often simplified versions or analytical solutions of eq. 1 are used. The gaussian plume model in all its variations is one of the possible analytical solutions when certain conditions are fulfilled like homogeneity of the surface and flow, stationarity of the atmosphere and windspeeds above 1 $m.s^{-1}$. The direct solving of eq. 1 allows for rather straightforward incorporation of other processes like chemical conversions, inhomogeneous flows, complex terrain, deposition and gas/particulate phase partitioning. These calculations can then be used to test parametrisations for use in simpler (gaussian plume) models. The K-model developed for our application is built to describe the dispersion due to a line source (a road) for several compounds and the influence of chemical reactions and gas/particulate phase partitioning in

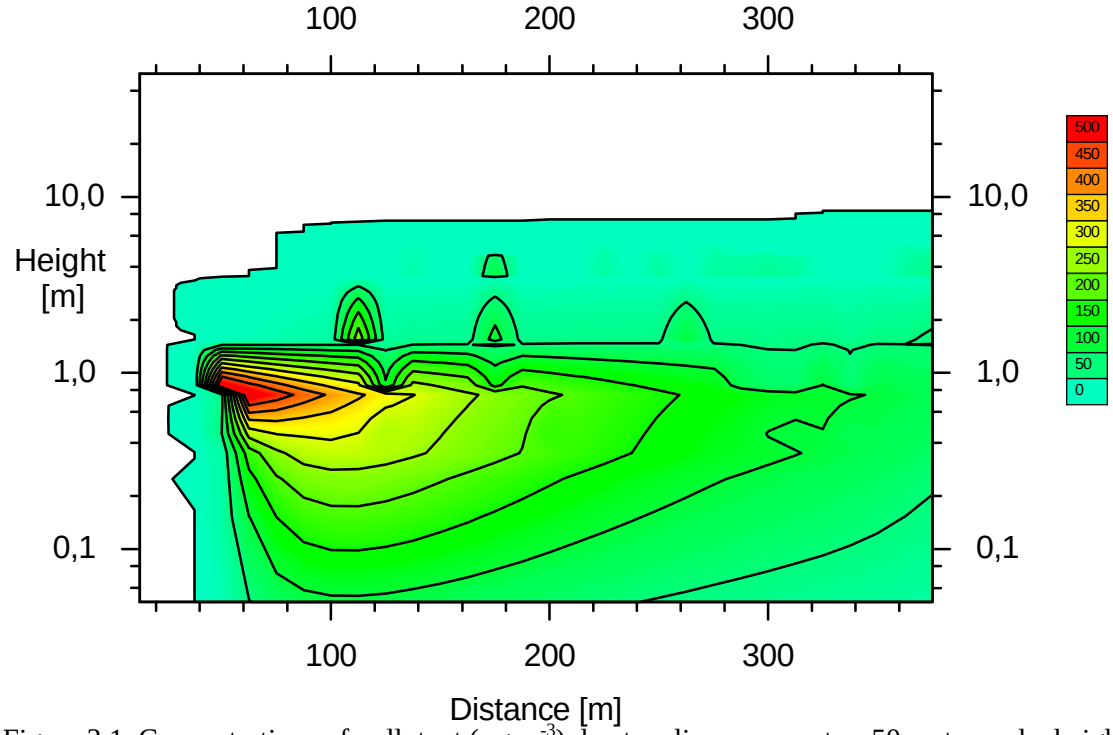

Figure 3.1 Concentrations of pollutant (µg.m^{-3}) due to a line source at x=50 meter and a height of 1 meter. Conditions as observed during the 23-9-98 A9 experiment. A deposition velocity of 1 cm.s^{-1} and a source strength of 1.10^{-3} g.m^{-1}.s^{-1} is assumed.

homogeneous and stationary conditions. The (photo)chemical reaction scheme and the description of the gas/particulate phase partitioning and aerosol size distribution and composition will be taken from other models like STEM-III, described later in this chapter. In figure 3.1 the calculated dispersion due to a line source of the K-model is displayed.
Large interactions between aerosol and gas phase can be expected (Wang et al., 1992; He et al, 1998). Processes that play a role are: emission, condensation, evaporation, coagulation, deposition and (heterogeneous) chemical reactions. All these processes have their own time scales. (Storey & Pankow, 1992). The K-model will allow to study which processes are important for the time and space scales at which experiments are performed and to test the simplified parametrisations in more detailed process studies and calculations.

3.2 Gaussian plume models

Gaussian plume models are widespread for use in regulatory purposes. They allow to describe the dispersion of pollutants in the atmosphere in a simple and straightforward statistical way. The width of the assumed gaussian shaped plume is determined by the standard deviation sigma per direction (x,y,z coordinates). The value of sigma depends on the time since release, height and the atmospheric stability. Several schemes exist to relate the sigma values to measured meteorological input. When detailed information is available, like in our experiment, detailed and more or less physical relations can be assumed between for example the measured friction velocity, Monin-Obukhov length and sigma, otherwise some intermediate or simplified assumptions have to be used to relate for example standard synoptic data to a guess of atmospheric stability.
The VLW (Voorspellingssysteem Luchtkwaliteit Wegtraces - Air Quality Prediction System for Road Tracks) model is designed for the evaluation by relevant authorities of the impact of new or changes in implementation of individual road systems in the Netherlands (DWW, 1999). It is based on the Car Special model from TNO (Duijm & Melle, 1992a+b). The model is built in principle around a gaussian plume model and is used for the calculation of long term mean and percentile concentration values at locations or at the face of buildings near the road to evaluate the possible exceedance of limit values for exposure to pollutants. The impacts of the layout of the road (taluds, tunnels), obstructions (sound limiting walls, buildings) and the photochemical reactions of NO_x are accounted for by using parametrisations developed by TNO (Duijm & Melle, 1992a+b). Only a limited number of parameters such as wind direction, wind speed and one Pasquill stability class (D) is taken into account.
For the evaluation of the results of a road experiment we will have to evaluate a plume averaged over several hours instead of the outcome of a statistically divided number of plumes per wind direction, stability and wind speed class, covering the period of a season to several years. The gaussian plume formula for a ground surface deflected plume due to a line source is:

$$f = \frac{1}{DP * \sqrt{2\pi} * \sigma_z * u}\left(e^{-\left[\frac{-(z-H)^2}{2*\sigma_z^2}\right]} + e^{\left[\frac{-(z+H)^2}{2*\sigma_z^2}\right]} \right) \qquad \{2\}$$

$C = f * Q$

C=concentration $(g.m^{-3})$

f=dispersion factor $(s.m^{-2})$

σ_z=dispersion coefficient (m)

u=windspeed $(m.s^{-1})$

z=measurement height (m)

H=source height (m)

Q=source strength $(g.m^{-1}.s^{-1})$

DP = Davenport correction

The formula used in VLW is a simplified version of this formula without the deflection term (the second e-power term in eq. 2).

The influence of vehicle movement, road dimensions, road shoulder height, influence of buildings etc. on the dispersion is accounted for by assuming an initial dispersion, following a set of rules developed for the Car Special model. This sigma value is enforced to the model by calculating a virtual source distance further away than the real source, so that correct initial dispersion at x=0 will be achieved.
The dispersion coefficient sigma-z in eq. 2 is dependent on the atmospheric stability and on the travel time and thus on the distance from the source. Sigma-z is evaluated in the VLW model for stability class D as a function of x. To evaluate the concentration measurements of our experiment a short term calculation was performed making use of the available meteorological information for maximum precision. Therefore the sigma-z values were calculated using the more refined set of calculations (utilizing the measured u_* and Monin-Obukhov length L) defined for the New National Model (Projectgroep, 1998).
In figure 3.2 the calculated dispersion is depicted as a function of downwind distance to the road axis under the conditions of the road experiment described in chapter 4. When no initial dispersion is assumed the dispersion follows a tailed bell shape, but with initial dispersion (in this case 2.75 meter) a slow decay function is calculated, with only a small difference between the results of the VLW and the National Model calculations, due to the fixation of the dispersion factor at x=0.

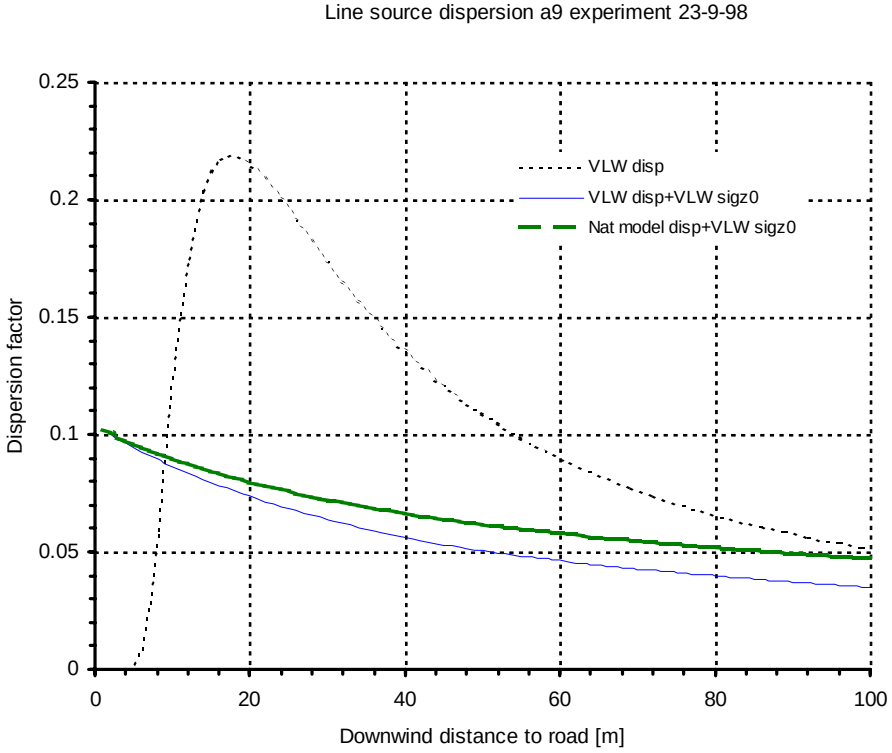

Figure 3.2 Calculated dispersion factor f (see formula 2) of pollutant due to a line source under the condition of the A9 road experiment as a function of downwind distance to the road. Shown are dispersion factors using the VLW dispersion and national model dispersion coefficients, with and without taking into account initial dispersion due to the road characteristics

If the influence of traffic on VOC concentrations and aerosol particle number and composition is to be evaluated with models like VLW, a separate parametrisation scheme has to be developed to translate the complex processes already described to a usable and reasonably accurate simple scheme. By coupling measurements and more complex models it will be possible to make a selection of those processes that at least to be accounted for in the VLW model to evaluate also the VOC and aerosol concentrations within the conditions of this model.

3.3 The ATHENS model

The simulation model ATHENS is a one-dimensional tropospheric chemistry model that simulates emissions of trace gases at the surface, vertical dispersion through diffusion and convection, photochemical conversions (Gery et al, 1989; Atkinson, 1990), wet and dry deposition, and horizontal transport (Viras L.G. and Siskos P.A., 1992). The troposphere is in the model divided in 12 layers. The simulation is controlled by physical parameters such as temperature, humidity, cloud parameters and photochemical reaction constants. The model can be used in different modes, representing different strengths of the simulated ozone precursor emission regimes: background, polluted and heavily polluted mode. A number of processes can be varied in intensity, this includes for example the emissions, the vertical diffusion and convection. This allows the model to be used for investigation of the effects of emissions of ozone precursors on the levels of the ozone concentration and demonstration of the effects of meteorological parameters on vertical dispersion and chemistry of trace gases. The model does not explicitly model aerosol size distribution and composition.

3.4 The Urban Airshed Model (UAM)

This model is appointed by law in the US to be used by the individual states to evaluate the production of photochemical smog due to antropogenic and biogenic emissions of air pollutants. Version 2.34 is available through the EPA web-sites. The UAM model is a full-blown Eulerian regional transport model with coupled chemistry using the CBM-III (Gery et al, 1987) scheme. The system consists of a myriad of programs for pre-processing of emission data, meteorological input data and post-processing of the output files. The code is highly dependend on the US coordinates and data formats, so that conversion of the model for use in our foreseen applications turned out to be a major job. The model is also of a somewhat older generation and doesn't provide any explicit scheme for the gas phase-particulate partitioning, so the conversion path was abonded quite soon.
A more current version of the UAM model (using the CBM-IV chemical scheme (Gery et al., 1989) and with a simple gas-particulate phase partitioning is not available for use outside the US, development of this model is continued.

3.5 The STEM-III model

The model selected as suitable for the detailed calculations is the box-STEM III model with included SCAPE code (Carmichael et al., 1986, 1991, 1994). The SCAPE sub-model considers a gas-particulate thermodynamic distribution of volatile species (Kim et al, 1993a, 1993b, 1995). The STEM III code was kindly provided to ECN in February 1999 by Dr. Carmichael of the State University of Iowa. In the near future parts of the SCAPE code will be incorporated in the K-model (see section 3.1) and be used to evaluate the measured concentrations and to derive and test the parametrisation development for use in gaussian plume models like VLW and to study in detail the behaviour of aerosols and VOCs in the first minutes after release into the atmosphere.
The STEM-III model includes 84 chemical species (56 long-lived, 28 short lived: pseudo steady state), 178 gas-phase and 31 aqueous phase reactions.
Simulations using this model have shown that interaction of aerosols with the ozone cycle may be as important as NO_x and VOC emissions in evaluation of ozone production (He et al., 1998).

4. EXPERIMENTAL RESULTS

4.1 Experiment layout

At 23-9-1998 an experiment was conducted at the A9 highway, near to Spaarnwoude, The Netherlands. The results of the measurements are presented in this chapter. Figure 4.1 gives some photographs of the experimental setup.
The location used was the A9 highway from Haarlem to Alkmaar, km 44.1, running from North to South. The mean traffic density during the measurement period was 6360 vehicles/hr (5% heavy traffic), maximum speed 120 km/h. We installed 3 measurement points, one (background) at east of road at 30 meters, two (polluted by the traffic) points at 10 resp. 35 meters west of road (See Fig. 4.2). The instrumental setup is depicted in fig. 4.3. Traffic density during the measurements as measured by the road authority is shown in figure 4.4.

Figure 4.1 Photographs of the 23-9-98 A9 experiment. The above picture shows from left to right the SMPS/CPC combinations, the LAS-X and NOx monitors and the Sierra HVS impactor. The down-left picture shows the Sierra HVS, the PUF/Filter device and the Berner impactor. The down-right picture shows the meteo mast at 35 meter of the road with on top the Solent sonic anemometer, the NOx monitor and the data logging hardware.

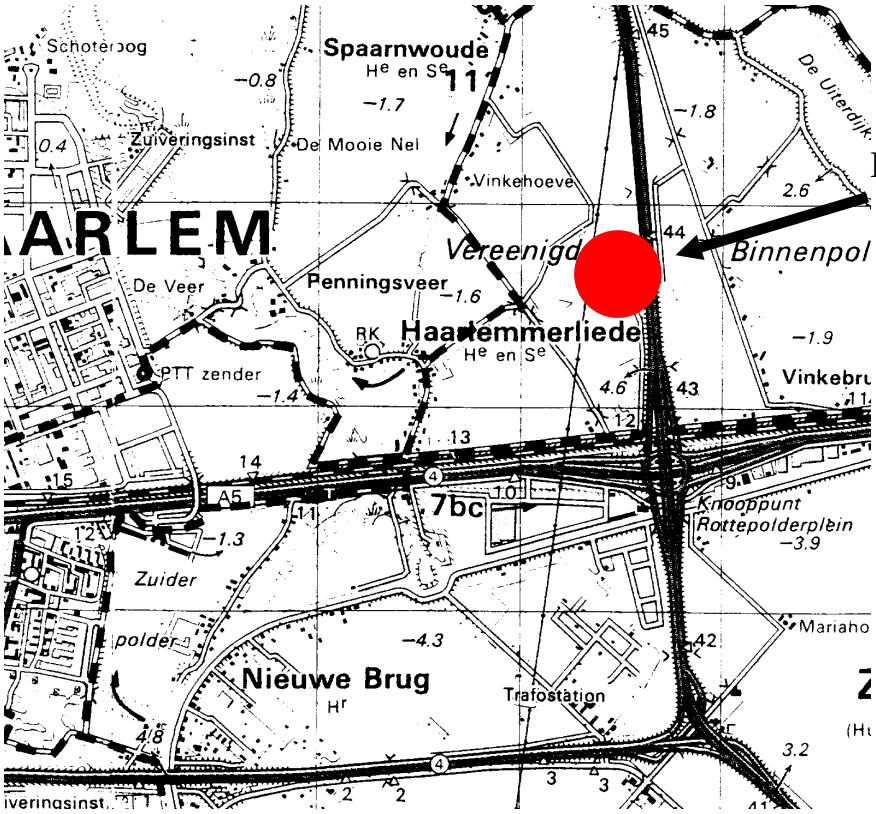

Figure 4.2 Situation map of the area of the A9 field experiment of 23-9-98.

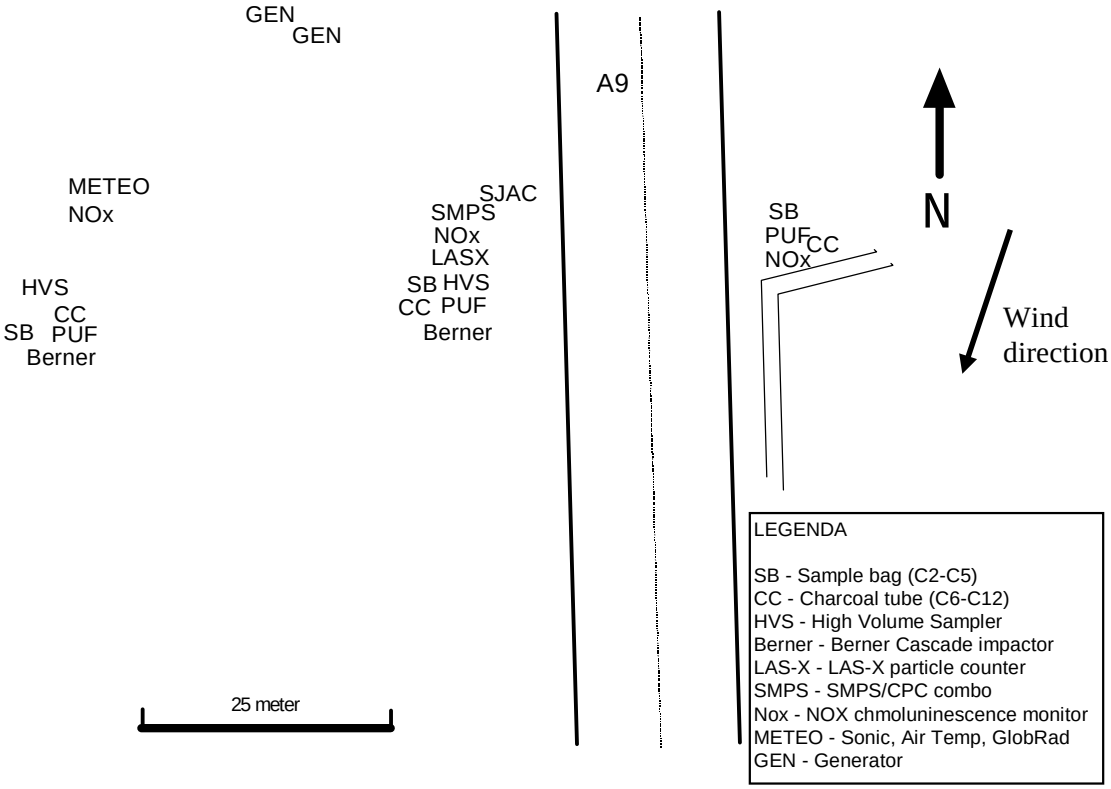

Figure 4.3 Location of the sampling equipment during the A9 field experiment of 23-9-98.

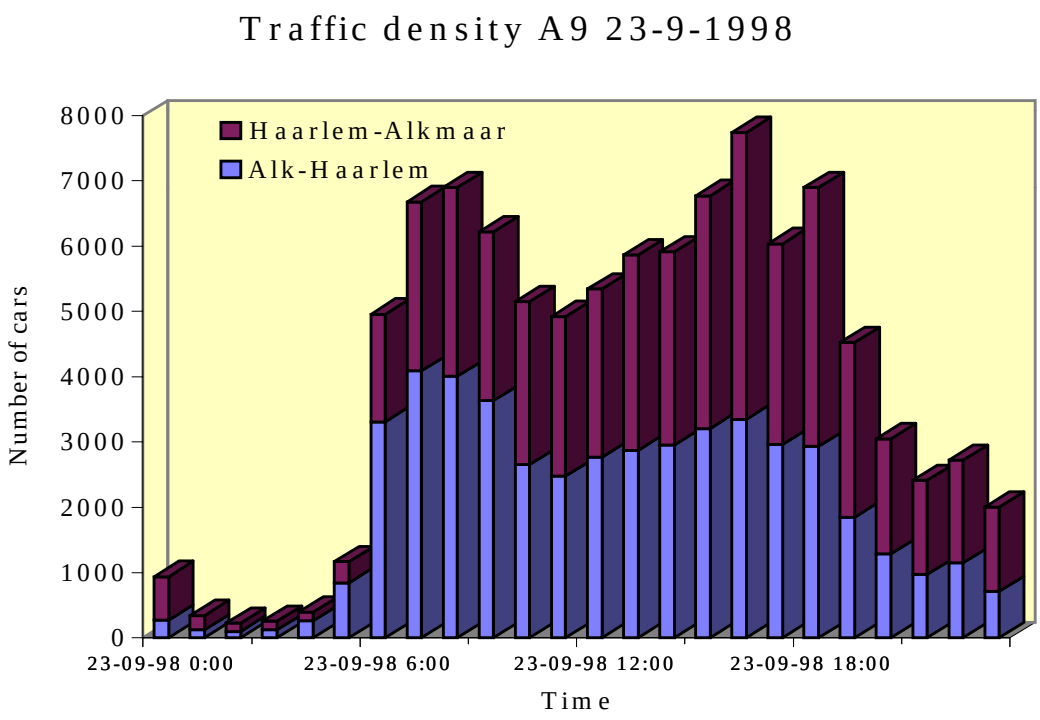

Figure 4.4 Traffic density on the A9 road at 23-9-98 as a function of time and travel direction.

Meteorological situation: A high pressure area over NW-Europe provided easterly winds with a cool night and a sunny day. The morning started with dense fog, that disappeared at about 11 pm (CEST). Thereafter almost clear conditions prevailed (some haze) with a global radiation maximum of 250 $W.m^{-2}$. Measurements started around 12 pm. Wind speeds were moderate and quite constant around 3-4 $m.s^{-1}$, the mean wind speed was 3.3 $m.s^{-1}$. Atmospheric stability was slightly unstable (Pasquill class C, Monin Obukhov length -54 meter). Winddirection unfortunately deviated from the forecast and varied from 0-40 ° and was almost parallel to the road around 13:30 and during the end of the experiment (see figure 4.5; table A10).

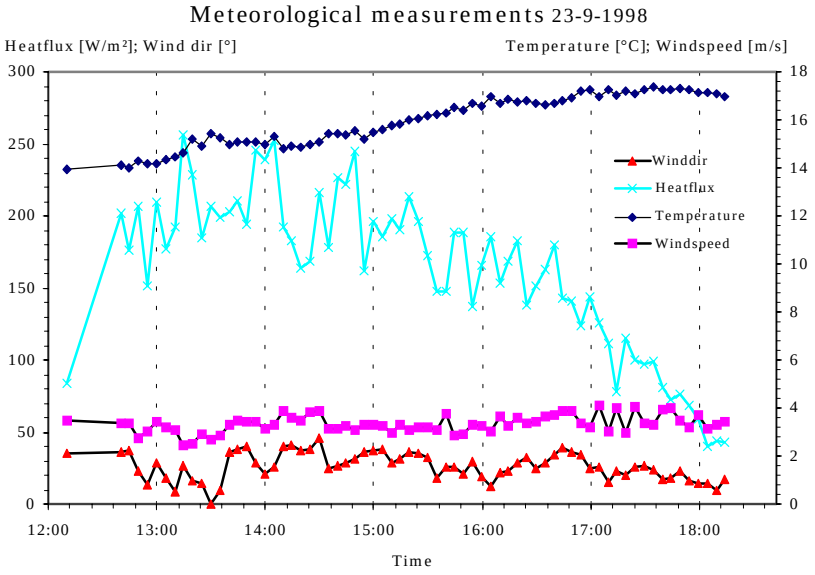

Figure 4.5 Meteorological measurements of the A9 experiment at 23-9-98. Shown here are the wind direction, wind speed, air temperature and the sensible heatflux as a function of time.

4.2 Gaseous compounds

C1-C5 measurements: VOC's consisting of 1 to 5 carbon molecules were sampled using sample bags, which were filled during the experiment at the 3 horizontal gradient locations. Analysis of the air was performed by GC-MS. The 12 most important compounds were identified. The concentration gradient, with the highest concentrations found at the 35 meter point does not follow the expected curve for most compounds (figure 4.6; table A7). The background measurement of 1-butanol shows an unexplained high value. Higher concentrations due to the traffic can be seen most clearly for acetaldehyde, ethanol and 2-butanone. The ethanol concentration is probably enhanced because of the cleaning of car windscreens, popably because of the high emission heights this leads to highest concentrations at the 35 m point. Benzene data is included in the next picture to illustrate the loss of this compound (and other $>c_6$ compounds) in bag samples. The concentrations shown were calulated assuming a detector response for all gases equal to that of the available standard of ethane. This can

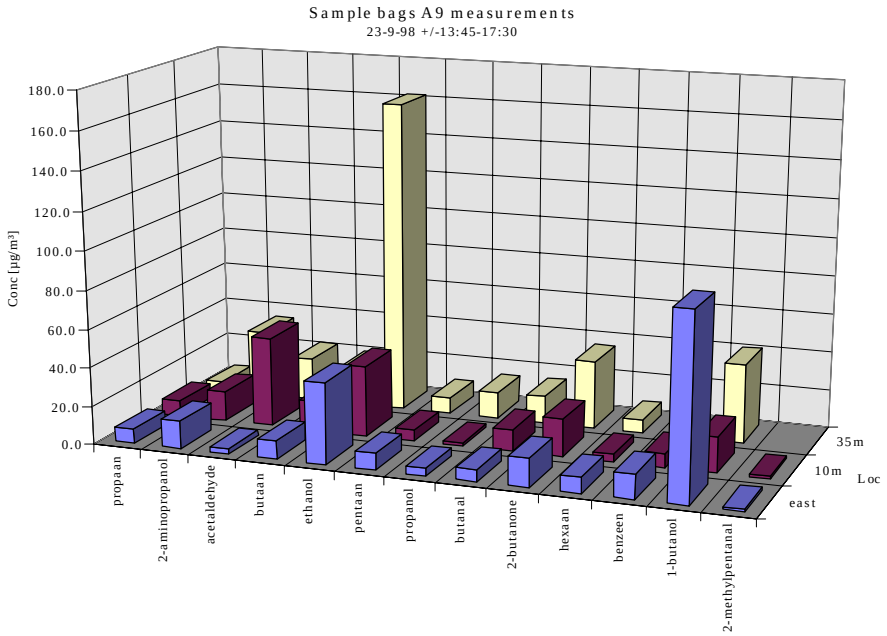

introduce a systematic error in the concentrations for components other than ethane of about 20%.

Figure 4.6 Concentrations of VOCs in the sample bags using GC-MS analysis

C6-C12 measurements: VOC's consisting of 6 to 12 carbon molecules were sampled using glass tubes filled with coconut charcoal, which were loaded at all three locations during two successive periods of about 3 hours. After extraction with CS_2 the samples were analysed by GC-MS. The concentration gradient for most compounds follows the expected pattern. Highest elevated concentrations are seen for 2 propenoicacid,2 methylester, benzene, toluene, 1-ethyl,2-methyl benzene, o/m xylene and p-xylene (figure 4.7). The second period shows higher concentrations due to higher traffic intensity and more neutral conditions (figure 4.8; table A8).

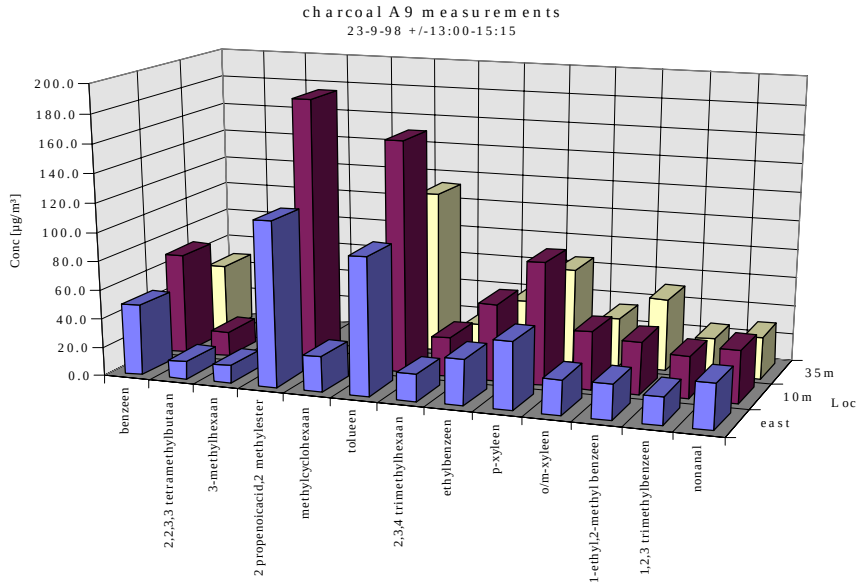

Figure 4.7 Concentrations of the most prominent VOCs in the charcoal tubes using GC-MS analysis for the first measurement interval

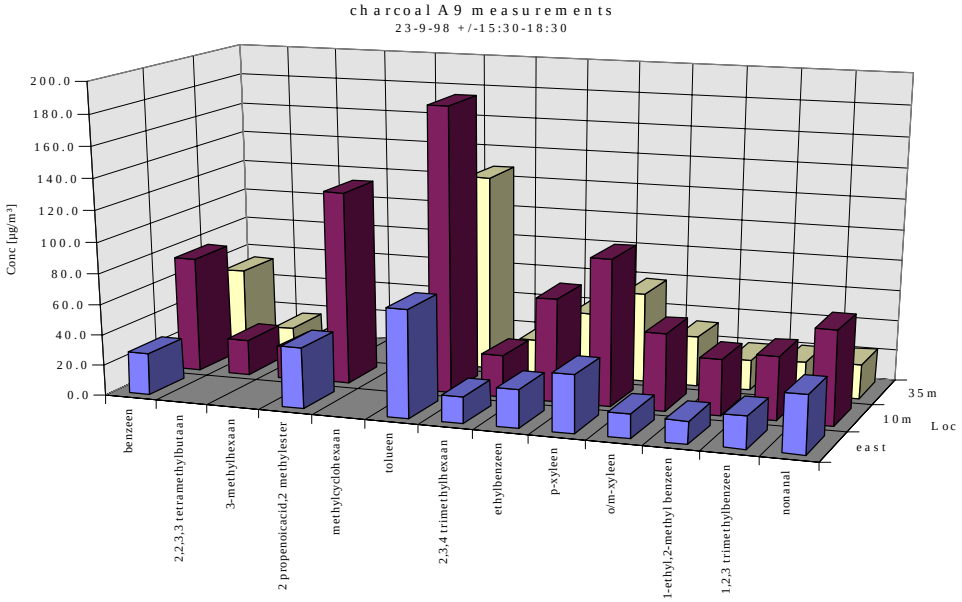

Figure 4.8 Concentrations of the most prominent VOCs in the charcoal tubes using GC-MS analysis for the second measurement interval

NO_x: NO_x concentrations were measured with standard chemoluminescent gas monitors. A clear elevation of the background concentration of 30-40 ppb could be detected with off-road levels of 80-100 ppb, here also higher concentrations were found at the larger distance, with peaks at 15:00 and 16:30, at these moments the winddirection was 40°, propably leading to an influence of NO_x emissions of the power generators on the measurements at the 35 m point. Traffic contributes as expected mainly to the NO levels, no conversion to NO_2 could be

detected in the small distance of the gradient, as can be seen in the figure 4.9. The upwind NO_X monitor results are not shown here due to malfunctioning of this monitor.

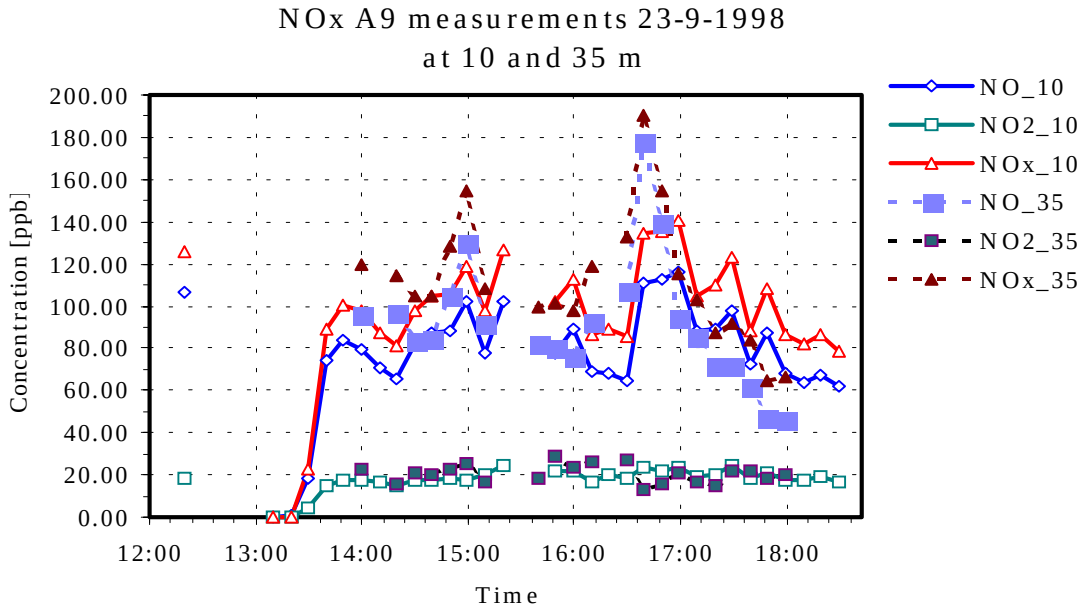

Figure 4.9 Concentrations of NO, NO_2 and NO_x at the downwind side of the road.

4.3 Aerosol sampling

Impactor measurements: Two Berner and three Sierra cascade impactors were employed to collect aerosols. The Sierra filters were analysed for heavy metals (ICP) (fig 4.10; table A9) and PAH's (HPLC) (fig 4.11; tables A4-A6). For PAH, only the compounds Phenanthrene, Pyrene, Benz[a]antracene, Chrysene, Benzo[a]pyrene and Benzo[k]fluoranthene could be detected at all stages of the impactors (Fig. 4.11a,b,c). Phenanthrene and Pyrene are bound to the more coarse particles, while elevated concentrations are found for Benzo-a-pyrene and Benzo[k]fluoranthene on the backup filter, which means that these compounds are bound to the smaller particles (<500 nm). Fluoranthene was only detected on the backup filter in high concentrations. The highest concentrations are found at the site further away from the road (35m).

Total aerosol mass (16, 68 and 77 µg.m-3 at resp. east, 10m and 35 meter positions) and the particle size distribution of Sierra's compare quite well with that of the Berner impactors (58 resp. 75 $\mu g.m^3$, Fig. 4.10). Here also the more remote sample point had highest concentrations, a small amount of extra mass was detected here for the small particles (<200 nm) as well as for the more coarse particles (around 5 µm).

Clear contributions of traffic to the levels of Zn, Pb, Cu and to less extent Cr can be seen, especially in the smaller sizes (<500 nm; see figure 4.10a,b,c).

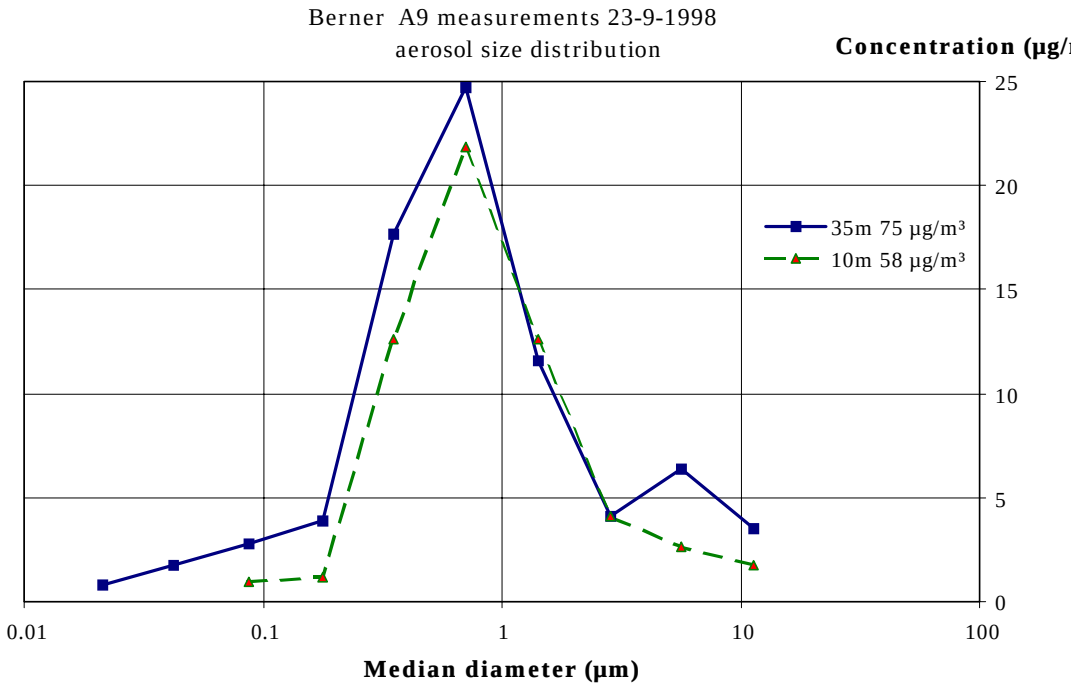

Figure 4.10 Berner impactor aerosol size distribution gradient

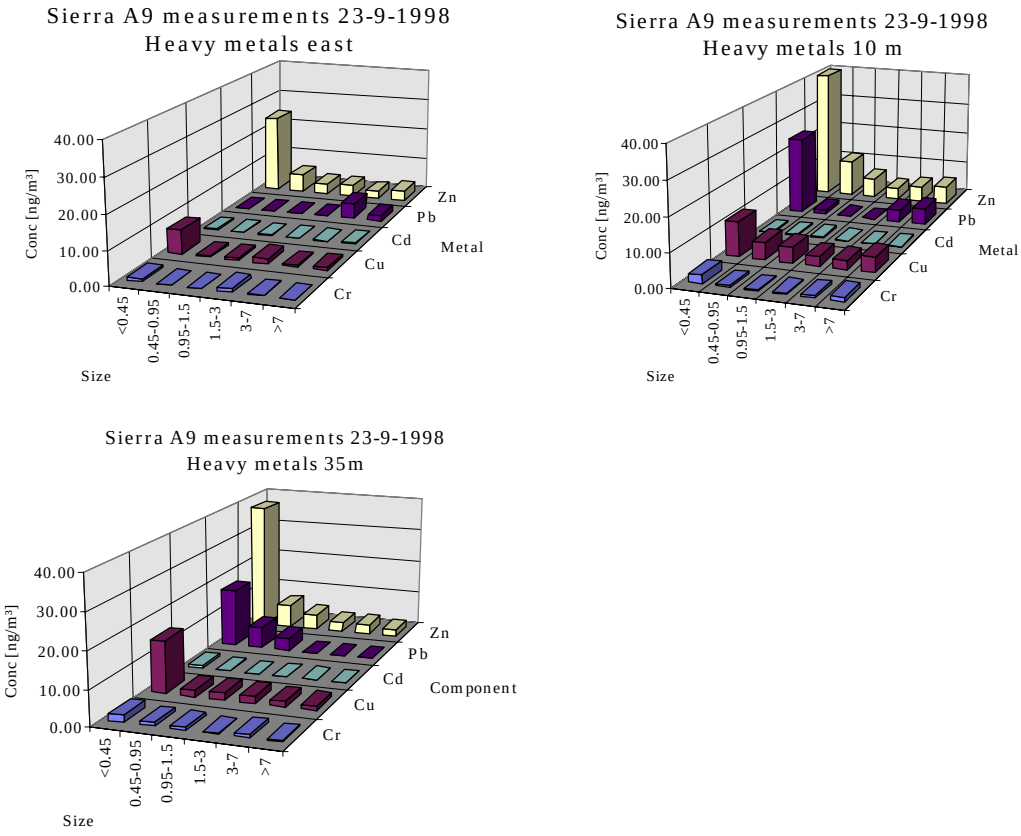

Figure 4.11 Sierra HVS concentrations of metals as a function of aerosol size

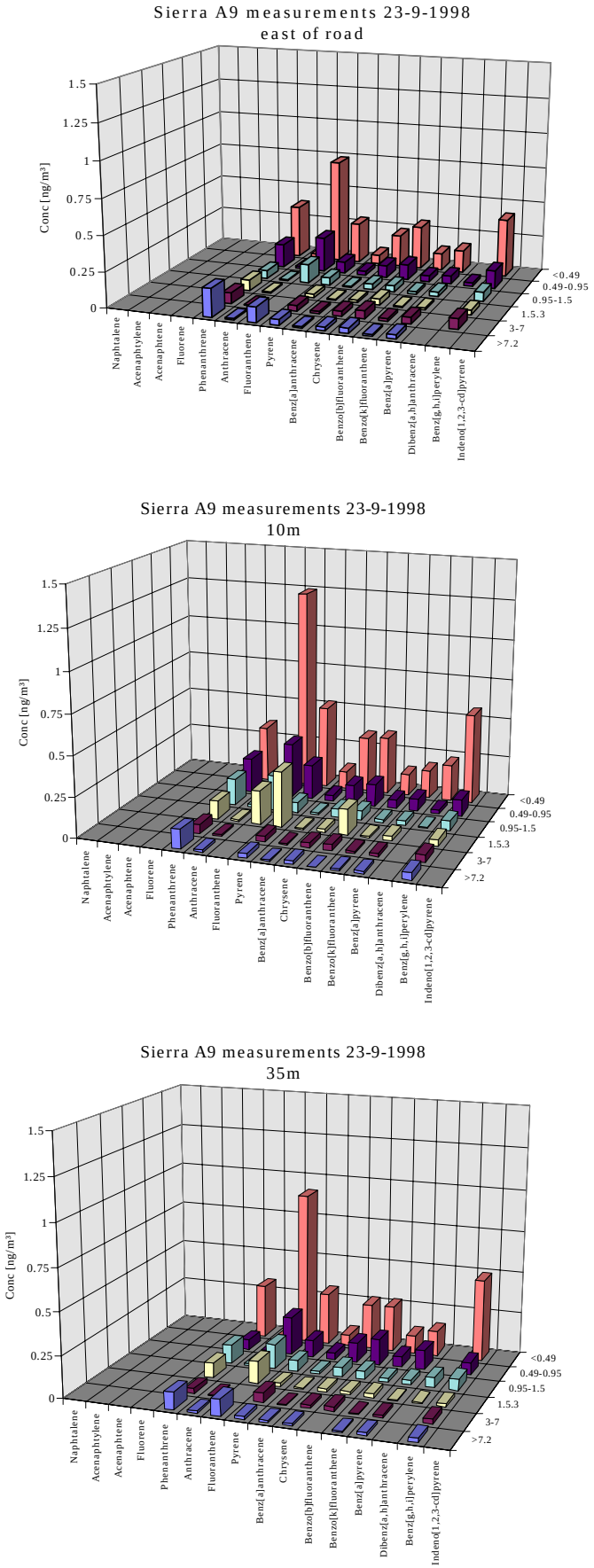

Figure 4.12 Sierra HVS concentrations of PAHs as a function of aerosol size

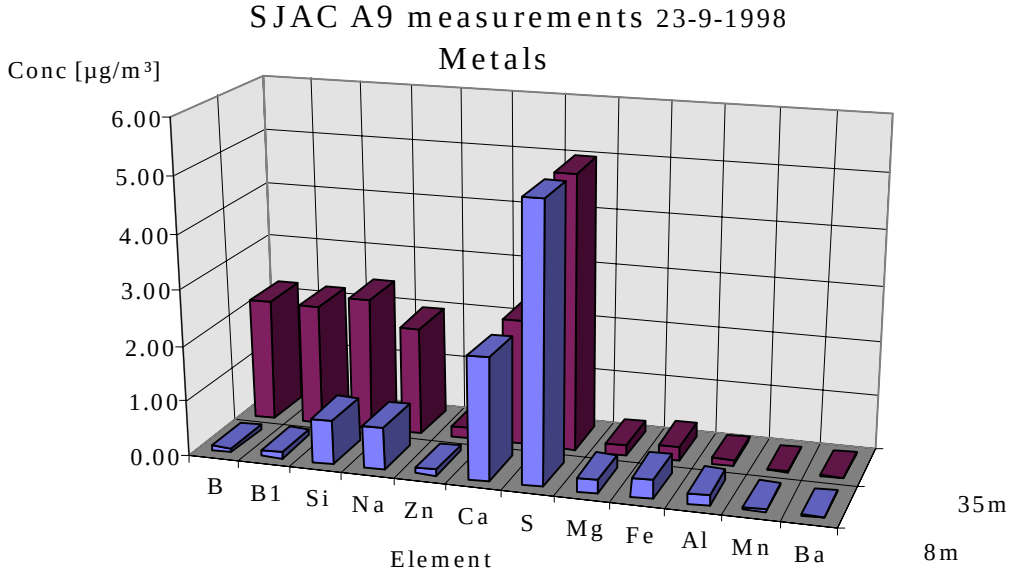

Figure 4.13 SJAC measurements of metals in aerosols

SJAC: The Steam Jet Aerosol Collector collected at the 10 and 35 meter locations total aerosol mass. The 20 minute samples were analysed for a large number of metals. Fig 4.13 shows the concentration results of the concentrations above detection level. Higher levels were found at the 35 meter point compared to the 10m point for B, Si and Na. All other metals of concentrations above the detection limit showed no significant difference. About 15% resp. 22% of the total aerosol mass was identified by the SJAC as metal at 10 and 35 meter.

PUF-samples: Polyurethane Foam/Filter combinations were employed at all three locations in two time intervals of about three hours to determine gaseous PAH components. Analysis for PAH's was performed by HPLC. The measured concentrations show a reversed gradient from 10 to 35 meter. High contributions of the traffic are seen here for fluorene, phenanthrene, antracene, fluoranthene and Benz[g,h,i]perylene. 1 to 30% of the PAH is found to be bound to the aerosol phase, the rest is gaseous. The results are show in figure 4.14 and table A3.

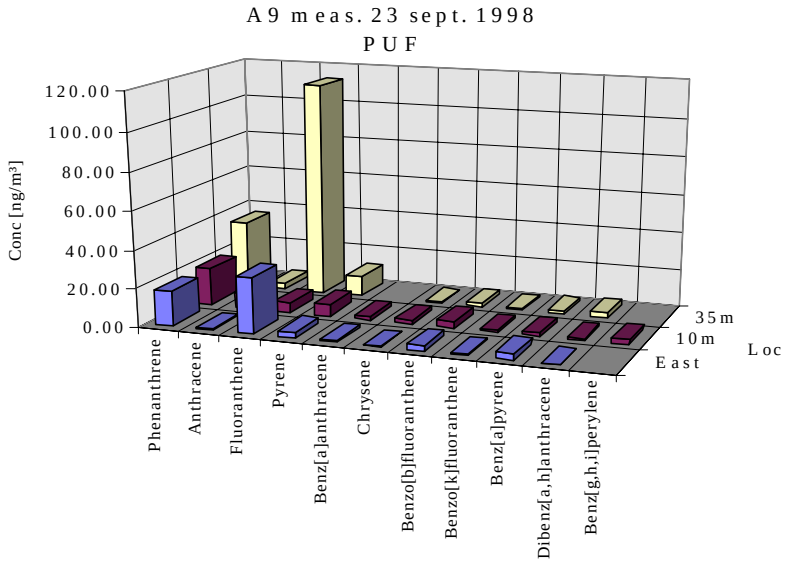

Figure 4.14 PUF/Filter combination measurements of total PAH

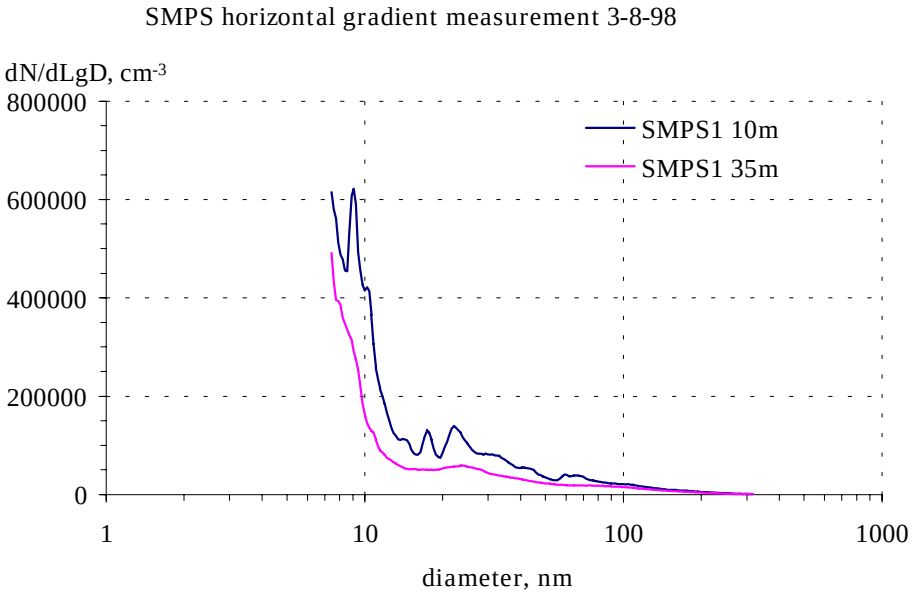

Figure 4.15 Aerosol size distribution gradient during the A9 3-08-98 experiment.

4.4 Aerosol size distribution measurements

On August 3, 1998 an explorative experiment was performed at the A9 measurement location to see whether the horizontal gradient in aerosol number distribution was strong enough to be detected by the SMPS/CPC combination. The windspeed was that day moderate and from the West, so the gradient was measured at the east side of the road. Figure 4.15 displays the measured aerosol number distribution a distance of 10 and 35 meter from the road. The ratio between the aerosol number concentration on the 35 and the 10 meter point depends on size and started with a factor of about 2 at sizes of 8 nm and went to a number of 1 for sizes of 100 nm and more. The horizontal gradient in aerosol number could be detected quite clearly by the measurement system.

On September 23, 1998 two SMPS/CPC systems and a LAS-X system were used. Instrumental and power quality problems however caused that just one of the SMPS/CPC systems started working as late as 16:30, the LAS-X system started working around 15:00. These problems did not allow for the simultanuous measurement of aerosol size distribution at two locations in a horizontal gradient as was planned on beforehand. It was decided to use the remaining time to measure with SMPS/CPC and LAS-X just at the 10 meter point closest downwind of the road. Figure 4.15 shows the measured average aerosol number distribution measured in the last hour of the experiment. Number concentrations were as high as on August 3, 1998. Normal high background values (for easterly winds) are a factor of ten lower then the values measured here, so the contribution of the vehicle emissions to the aerosol number concentrations is detected here quite clearly. Figure 4.16 compares the aerosol mass distribution estimated from the LAS-X system (assuming a density of 1.77 g/l) with that measured by the Berner impactors. A clear resemblence can be seen, allthough the LAS-X distribution shows a more marked peak at 500 nm. This is caused by the somewhat overlapping characteristics for the impaction on the subsequent impactor stages, which leads to a somewhat flattened distribution for the impactors. The results show that the optical methods like CPC/SMPS and LAS-X lead to similar results as the more conventional methods while also providing more detailed and higher time-resolved information on aerosol size distribution

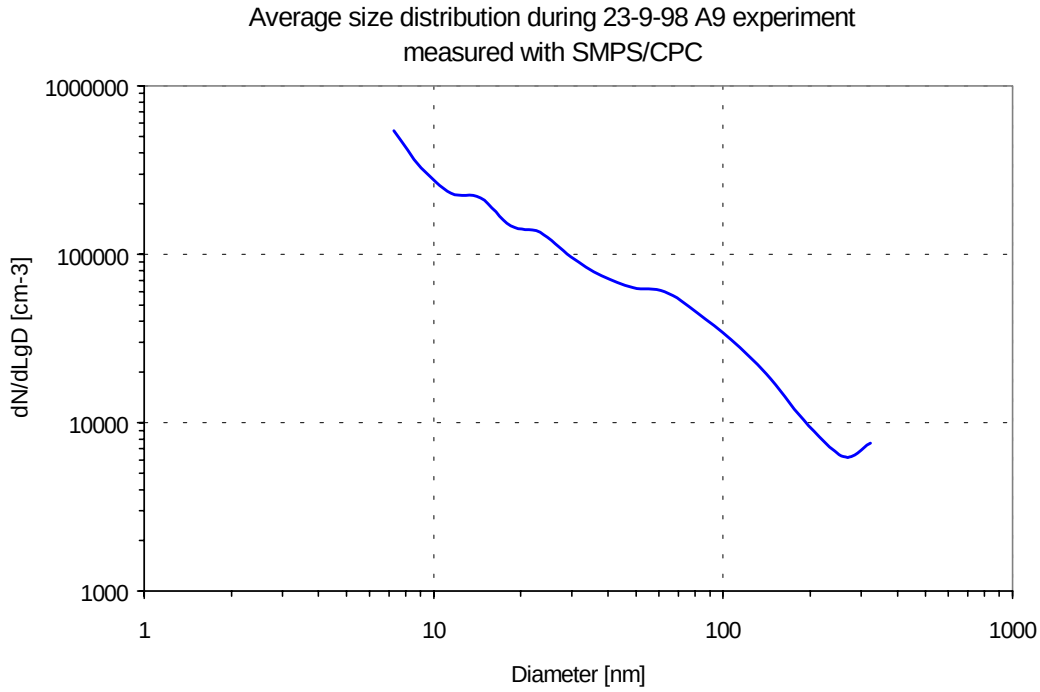

Figure 4.16 Aerosol size distribution at the 10 meter point during the A9 23-09-98 experiment. Normal background aerosol number concentrations are 20,000-30,000 particles.cm^{-3}

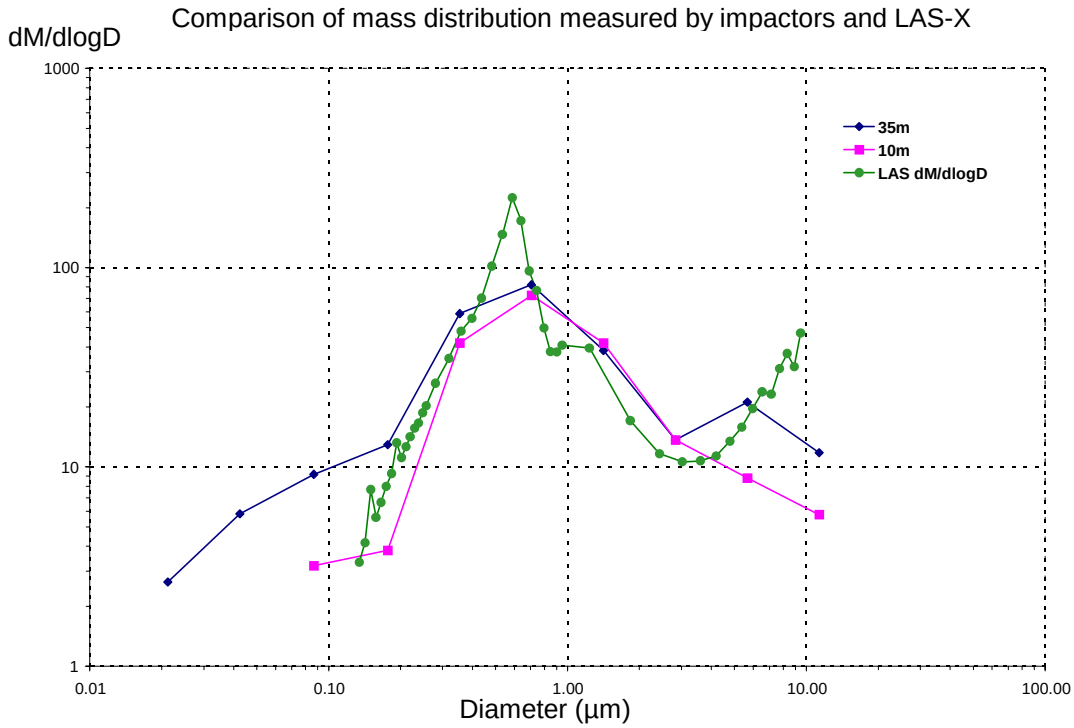

Figure 4.17 Comparison of the aerosol mass distribution measured by the Berner impactors and by the LAS-X instrument during the A9 23-09-98 road experiment.

4.5 ^{14}C measurements

After 3 hours of sampling the recovery of the ^{14}C BAP in the PUF/filter measurements is 100%. The recovery of BAP in the HVS after 6 hours of sampling is 52%. After 40 hours of sampling the recovery is only 20%. This means that the high volume sampler technique is not very adequate for measuring the chemical partitioning of the aerosols in the different size classes. When short sample periods are used the the results obtained can be used as indicative values but then the relative measurement errors are large due to the detection limit of the chemical analysis systems. When larger sample times are used the recoveries are so low that the measurements give very little information. The PUF/Filter combination shows an excellent recovery.

4.6 Calculated traffic emissions

By combining the emission factors of the gaussian plume model of section 3.2 with the concentration data the emission strengths for several components can be evaluated. The results of the PUF and bag samples are not used here because of the inverted concentration gradient for most components, which is for the PUF plugs propably due to an analytical problem in one of the two PUF cartridges. Of the HVS only the concentrations on the backup filter are used as these will contain most of the material emitted by the traffic and because the concentrations on the backup filters are well above the detection limit for most PAH's.
The resulting emissions for selected components is shown in table 4.1. For calculation of the dispersion factors the average meteorological conditions were take from three periods, one from 12:00-15:00, one from 15:00 to 18:00 and one from 12:00 to 18:00, corresponding approximately in time with the sampling intervals of the different concentration samples.

	concentrations ($ng.m^{-3}$)			fluxes ($ng.m^{-1}.s^{-1}$)			µg per km
Name	**c back**	**c 10m**	**c 35m**	**flux 10m**	**flux 35m**	**avg. flux**	**Emission**
Fluoranthene $PM_{0.5}$	0.7	1.2	0.9	8.4	5.0	6.7	3.6
Chrysene $PM_{0.5}$	0.2	0.3	0.3	1.8	1.1	1.5	0.8
Benz[ghi]perylene $PM_{0.5}$	0.4	0.6	0.5	2.4	2.2	2.3	1.3
Toluene[1]	95	161	113	1016	455	735	427
Toluene[2]	70	184	128	2012	1775	1900	990
Benzene[1]	49	70		330		330	192
Benzene[2]	27	76	54	851	821	836	437
p-xylene[1]	47	85	66	590	499	544	317
p-xylene[2]	37	95	59	1007	651	829	433
o/m-xylene[1]	24	40	34	251	252	251	146
o/m-xylene[2]	16	50	32	598	505	551	288
123 trimethylbenzene[1]	19	30	25	159	156	158	92
123 trimethylbenzene[2]	20	41	21	363	18	191	100
Cu PM_7	10	26	22	279	365	322	174
Cr PM_7	1.5	4	4.9	49	102	76	41
Zn PM_7	39	68	54	511	478	495	266
Pb PM_7	0	26	26	576	787	621	336

Table 4.1 Measured horizontal concentration gradients and calculated vehicle emissions for selected components during the A9 experiment of 23-9-1998.
[1] = period 12h-15h; [2] = period 15h-18h;others period 12h:18h

Except for benzene the emissions per car are within a factor of two when the two subsequent sample intervals are considered. Except for toluene in the first period and trimethylbenzene in the second period the fluxes calculated from the measured concentration at the 10 meter and the 35 meter point differ less then 50%. The use of two sample periods and two sample points allows to estimate the precision of the calculated emissions. So the error in the emissions

shown in table 4.1 is about 50%. Systematic errors due to calibration error in the chemical analysis cannot be accounted for by this method however.
The literature states emissions higher than the ones measured here. CBS (1990) reports Pb emissions of 2200 µg.km^{-1} for this type of highway, which is higher by a factor of 7. For benzene emissions of 15000 µg.km^{-1} are given, which is substantially higher than the emission found here.
The fact that the concentrations for benzene found in the experiment are lower than those of toluene indicates that the calibration of the charcoal samples needs more attention, as the emissions rates from traffic of toluene are expected to be much smaller as those of toluene, but as the meteorological conditions during the experiment were far from optimal, emission estimates from this experiment should not be considered as reliable in the first place.

4.7 Conclusions

Disturbances by the emissions of the power generators because of the unexpected wind direction during the experiment disables the use of the measurements in this report to derive emission estimates of highway traffic. The use of a horizontal profile enabled us to detect this disturbance. When the measurements are repeated, the generators should be placed at a location downwind of the most downwind measurement location, if the situation allows this.
Of the gaseous compounds, p-xylene, benzene and toluene are good tracers for the traffic emissions. As PAH tracers Phenanthrene, Pyrene and Benz[a]pyrene can be used.
Sample bag, glass tubes with charcoal absorbents (gases), Sierra impactor (aerosol) and PUF methods (gaseous+aerosol PAH) as deployed here togehther with the used analysis techniques are suitable methods to evaluate the traffic emissions with regards to aerosols and gases.
SMPS/CPC and LAS-X measurements compare very well with the more conventional measurements techniques and also provide more detailed information on the aerosol size distribution, especially in the size ranges below 0.5 µm.
The HVS technique can be used to sample PAHs only when short sampling intervals in the order of several hours are used, otherwise recovery is too low. Chemical partitioning of the different aerosol size classes is only possible for short sampling periods, but to get results for all PAH's and impactor stages a lower detection limit is required then currently possible using the present equipment and methods.
In order to calculate reliable estimates of trafffic emissons more attention is needed in the calibration of the analysis techniques.

5. DISCUSSION

Optical methods like CPC/SMPS and LAS-X lead to similar results as the more conventional methods for the size distribution of aerosol mass while also providing more detailed and higher time-resolved information on aerosol size distribution.
Determining accurately the chemical composition of different aerosol size classes is still very difficult. A compromise has to be found between the need to collect a minimally needed mass for accurate analysis above detection limits, the time-resolution required, avoidance of sample deficiencies because of flow rates, chemical reactions etc. In priciple the chemical analysis of the different aerosol size classes is possible, but with high demands on labour and precision of the field workers.
As the errors in concentrations measurements of PAHs and VOC are rather large and the difficult sampling of aerosols also leads to uncertainties in the order of 20-40%, concentration differences have to be large to be detected reliable. For higher accuracy also appropriate standards of the relevant VOC's will have to be obtained and employed in the GC/MS system in the future, allowing calibration factors per component.
Following the modelling results of section 3.1 and 3.2, future road experiments wil have to be carefully planned, with more distance between the locations for determining the horizontal concentration gradients (100-200 meter) to have concentration differences of a factor of 2 or more. Background measurements upwind as were deployed here are of course also very important.
Due to the wind direction being more parallel to the road axis than was expected during the experiment planning, the results of the concentration gradients measured during the 23-9-98 experiment were not satisfactorily. When the wind is almost parallel to the road, a small deviation in wind direction will change the 'virtual'distance x (proportional to cos α) to the road, thus influencing the dispersion factor quite drastically. This will lead to higher concentrations in reality then modelled when the average wind direction of a certain period is used due to the much lower dilution for small travel distances as for larger distances. This effect wil be larger for the 35 meter point as for the 10 meter sample point.
Another problem was the placement of the two power generators used for the experiment. As can be seen in fig 4.3 they were placed in the north-east direction of the 35 meter sample point. It is likely that the emissions of these generators have influenced the concentration measurements at the 35m sample point, especially in the period around 14:00h.
The particulate emissions of traffic are found in the smaller size fractions below 500 nm, as was expected. No significant horizontal gradient could be found in the total mass of aerosol. The experiment was carried out with easterly winds and continental, polluted air. The situation could be somewhat different when cleaner background conditions occur, for example with southwestely of northwesterly wind directions.
Determination of the change of chemical composition of aerosols due to traffic can be resolved best by just sampling the smallest size class possible of particles for which chemical analysis delivers a significant result (depending on detection limits). An attractive way to do this would be to use $PM_{2.5}$ separators, followed by a filter/PUF combination, this prevents the evaporative losses found in the Sierra HVS. Further optimisation of the GC/MS and HPLC analysis will be needed however and usage of standard commercially available and well characterised PUF plugs will be desirable, or more work will have to be invested in the standardisation, production and characterisation of the PUF plugs produced at the laboratory.

6. REFERENCES

Ackermann IJ, Hass H, Mennesheimer M, Ebel A, Binkowski FS & Shankar U, 1998. Modal aerosol dynamics model for Europe: development and first applications. Atm Env, 32, 2981-2999.

Atkinson R, 1990. Gas-phase troposheric chemistruy of organic compounds: a review. Atm Env, *24A*, 1-41.

Carmichael et al., 1986. Atm. Env., *20*, 173-188.

Carmichael et al., 1984. Atm. Env., *18*, 937-951.

Carmichael et al., 1991. Atm. Env., *25*, 2077-2090.

Gery MW, Whitten GZ, Killus JP & Dodge MC, 1989. A photochemical kinetics mechanism for urban and regional scale modelling. JGR, *94*, D10, 12925-12956.

He S, Carmichael GR, Sandu A, Hotchkiss B & Damian-Iordache V, 1998. Application of ADIFOR for air pollution model sensitivity studies. In: Proceedings APMS'98, october 1998.

Kaupp H & Umlauf G, 1992. Atmospheric gas-particle partitioning of organic compounds: comparison of sampling methods. Atm Env, 26A, 2259-2267.

Khlystov A, Wyers GP, Slanina J, 1995. The Steam-Jet Aerosol Collector. Atm Env, *29A*, 2229-2234.

Kim et al., 1993. Aerosol Sci. & Tech., *19*, 157-181.

Kim et al., 1993. Aerosol Sci. & Tech., *19*, 182-198.

Kim et al., 1995. Aerosol Sci. & Tech., *22*, 93-110.

Slanina J, Pio C, Koppmann R, Czapiewski K von, Larsen B, Kotzias D, Borg K van der, Tüdös A & Zwaagstra O, 1998. Determination of antropogenic and biogenic contribution to ambient volatile organic carbons. Petten, ECN, report ECN-C--98-081.

Peters A, Wichmann HE, Tuch T, Heinrich J & Heyder J, 1997. Respiratory effects are associated with the Number of ultrafine partciles. Am J Respir Crit Care Med, *155*, 1376-1383.

Storey JME & Pankow JF, 1992. Gas-particle partitioning of semi-volatile organic compounds to model atmospheric particulate materials-I. Sorption to graphite, sodium chloride, alumina and silica particles under low humidity conditions. Atm Env, *26A*, 435-443.

Projectgroep, 1998. Nieuw Nationaal model; verslag van het onderzoek van de projectgroep Revisie Nationaal Model. Den Haag, Infomil, ISBN 90-76323-00-3.

Viras LG & Siskos PA, 1992. Air pollution by gaseous pollutants in Athens, Greece. In: Gaseous pollutants: Characterization and cycling, edited by J.O. Nriagu, pp. 271-305, John Wiley & Sons, 1992

Wang SC, Flagan RC & Seinfeld, 1992. Aerosol formation and growth in atmospheric organic/NOx systems-II.Aerosol dynamics. Atm Env, 26A, 421-434.

APPENDIX A MEASUREMENT VALUES

Table A1 Summary of the measurement setup, samples times, flows and sampled volumes.

Measurement info	**A9 road experiment**					
Date:	**23-Sep-98**					
Location	**1**	**HVS**	**PUF**	**Char1**	**Char2**	**Bag1**
	100 m east of A9	**(m/min)**	**(L/min)**	**(ml/min)**	**(ml/min)**	**(ml/min)**
Sample code:		**HVS1K**	**PUF1K**	**1-1**	**1-2**	**loc1**
From:		11:46	11:47	11:47	14:50	11:47
To:		17:46	17:36	14:47	17:35	13:35
Sample time	(min)	360	349	180	165	108
Flow		119	54	585	450	141
Volume	(m^3)	364	18.8	0.105	0.074	0.0152
Location:	**2**	**HVS**	**PUF**	**Char1**	**Char2**	**Bag1**
	10 m west of A9	**(m/min)**	**(L/min)**	**(ml/min)**	**(ml/min)**	**(ml/min)**
Sample code:		**HVS2K**	**PUF2K**	**2-1**	**2-2**	**loc2**
From:		12:35	12:48	12:50	15:22	13:45
To:		18:30	18:24	15:20	18:22	17:15
Sample time	(min)	355	336	150	180	150
Flow		123	66	541	555	88
Volume	(m^3)	371	22.2	0.081	0.100	0.0132
Location:	**3**	**HVS**	**PUF**	**Char1**	**Char2**	**Bag1**
	30 m t.w. van A9	**(m/min)**	**(L/min)**	**(ml/min)**	**(ml/min)**	**(ml/min)**
Sample code:		**HVS3K**	**PUF3K**	**3-1**	**3-2**	**loc3**
From:		13:10	13:17	13:13	15:35	13:48
To:		18:47	18:47	15:33	18:45	16:30
Sample time	(min)	337	330	140	190	162
Flow		119	60	450	485	84
Volume	0.013608	341	19.8	0.063	0.092	

Table A2 Number of vehicles per hour on the highway A9 at km 37.3 (RWS, 1998)

nr of cars	direction	
Date/Time	Alkmaar-Haarlem	Haarlem-Alkmaar
23-09-98 0:00	272	666
23-09-98 1:00	122	222
23-09-98 2:00	101	127
23-09-98 3:00	124	128
23-09-98 4:00	264	128
23-09-98 5:00	844	324
23-09-98 6:00	3313	1647
23-09-98 7:00	4088	2593
23-09-98 8:00	4006	2892
23-09-98 9:00	3630	2589
23-09-98 10:00	2655	2496
23-09-98 11:00	2481	2441
23-09-98 12:00	2768	2574
23-09-98 13:00	2874	2993
23-09-98 14:00	2954	2956
23-09-98 15:00	3209	3564
23-09-98 16:00	3349	4391
23-09-98 17:00	2960	3079
23-09-98 18:00	2935	3965
23-09-98 19:00	1851	2675
23-09-98 20:00	1287	1764
23-09-98 21:00	973	1442
23-09-98 22:00	1146	1576
23-09-98 23:00	710	1293

Table A3 PUF/Filter concentrations of the 23-9-98 measurements (- denotes values below the detection limit).

(ng/m^3) Component	PUF East	PUF 10m	PUF 35m
Naphtalene	-	-	-
Acenaphtylene	-	-	-
Acenaphtene	-	-	-
Fluorene	-	-	-
Phenanthrene	18.44	20.17	35.43
Anthracene	0.81	8.29	3.28
Fluoranthene	29.48	5.27	112.94
Pyrene	3.11	6.21	10.57
Benz[a]anthracene	1.14	1.98	-
Chrysene	0.18	2.09	0.44
Benzo[b]fluoranthene	3.01	3.54	1.90
Benzo[k]fluoranthene	0.97	1.19	1.02
Benz[a]pyrene	3.44	1.63	1.88
Dibenz[a,h]anthracene	-0.40	0.88	2.68
Benz[g,h,i]perylene	-	2.47	-
Indeno[1,2,3-cd]pyrene		-	-
Sum:	60.17	53.72	170.14
"Gaseous"	51.84	39.94	162.23
"Aerosol-bound"	8.34	13.78	7.91
Ratio Aeros/Gas (%)	16.1	34.5	4.9

Table A4 Sierra HVS EPA-16 PAH concentrations of the 23-9-98 measurements at the east side (background) of the road (- denotes values below the detection limit).

(ng/m^3)	Size class (µm)					
	>7.2	**3-7**	**1.5.3**	**0.95-1.5**	**0.49-0.95**	**<0.49**
Component						
Naphtalene	-	-	-	-	-	-
Acenaphtylene	-	-	-	-	-	-
Acenaphtene	-	-	-	-	-	-
Fluorene	-	-	-	-	-	-
Phenanthrene	0.20	0.08	0.08	0.06	0.17	0.37
Anthracene	0.01	0.01	0.01	0.01	0.02	0.03
Fluoranthene	0.11	-		0.13	0.24	0.73
Pyrene	0.04	0.04	0.03	0.05	0.08	0.28
Benz[a]anthracene	0.01	0.02	0.007	0.01	0.03	0.06
Chrysene	0.02	0.04	0.02	0.04	0.09	0.23
Benzo[b]fluoranthene	0.04	0.06	0.043	0.04	0.11	0.30
Benzo[k]fluoranthene	0.01	0.02	0.01	0.02	0.04	0.12
Benz[a]pyrene	0.03	0.05	0.01	0.03	0.06	0.16
Dibenz[a,h]anthracene	-	-	-	-	0.02	-
Benz[g,h,i]perylene	-	0.07	0.033	0.06	0.13	0.412
Indeno[1,2,3-cd]pyrene	-	-	-	-	-	-
Sum:	0.47	0.37	0.23	0.46	0.98	2.70
"Gaseous"	0.36	0.12	0.11	0.25	0.51	1.42
"Aerosol-bound"	0.11	0.24	0.12	0.21	0.47	1.28
Ratio Aeros/Gas (%)	31	202	109	82	93	91

Table A5 Sierra HVS EPA-16 PAH concentrations of the 23-9-98 measurements at 10 west of the road (- denotes values below the detection limit).

(ng/m^3)	Size class (µm)					
	>7.2	**3-7**	**1.5.3**	**0.95-1.5**	**0.49-0.95**	**<0.49**
Component						
Naphtalene	-	-	-	-	-	-
Acenaphtylene	-	-	-	-	-	-
Acenaphtene	-	-	-	-	-	-
Fluorene	-	-	-	--	-	dtl
Phenanthrene	0.12	0.06	0.11	0.16	0.21	0.34
Anthracene	0.01	0.01	0.012	0.02	0.02	0.03
Fluoranthene	-	-	0.21	0.22	0.34	1.24
Pyrene	0.03	0.04	0.34	0.06	0.21	0.52
Benz[a]anthracene	0.0067	0.01	0.01	0.01	0.04	0.11
Chrysene	0.02	0.03	0.02	0.05	0.12	0.34
Benzo[b]fluoranthene	-	0.04	0.16	0.06	0.14	0.36
Benzo[k]fluoranthene	0.01	0.02	0.01	0.02	0.05	0.13
Benz[a]pyrene	0.02	0.02	0.03	0.03	0.08	0.17
Dibenz[a,h]anthracene		-	-	0.01	0.02	0.22
Benz[g,h,i]perylene	0.04	0.05	0.04	0.06	0.10	0.56
Indeno[1,2,3-cd]pyrene	-	-	-	-	-	-
Sum:	0.26	0.26	0.94	0.70	1.34	4.03
"Gaseous"	0.16	0.10	0.67	0.46	0.79	2.13
"Aerosol-bound"	0.10	0.15	0.27	0.23	0.55	1.90
Ratio Aeros/Gas (%)	60	150	40	51	69	89

Table A6 Sierra HVS EPA-16 PAH concentrations of the 23-9-98 measurements at 35 meter west of the road (- denotes values below the detection limit).

(ng/m^3)	Size class (µm)					
	>7.2	**3-7**	**1.5.3**	**0.95-1.5**	**0.49-0.95**	**<0.49**
Component						
Naphtalene	-	-	-	-	-	-
Acenaphtylene	-	-	-	-	-	-
Acenaphtene	-	-	-	-	-	-
Fluorene	-	-	-	-	-	-
Phenanthrene	0.10	0.03	0.09	0.11	0.06	0.32
Anthracene	0.01	0.004	-	0.01	0.01	0.02
Fluoranthene	0.10	-	0.13	0.15	0.23	0.91
Pyrene	0.02	0.05	0.02	0.06	0.10	0.31
Benz[a]anthracene	0.012	0.003	0.006	0.02	0.04	0.07
Chrysene	0.01	0.02	0.019	0.05	0.11	0.27
Benzo[b]fluoranthene	-	0.03	0.02	0.05	0.15	0.27
Benzo[k]fluoranthene	0.01	0.01	0.02	0.02	0.06	0.11
Benz[a]pyrene	0.02	0.01	0.01	0.03	0.12	0.15
Dibenz[a,h]anthracene	-	-	0.01	0.06	-	-
Benz[g,h,i]perylene	0.03	0.03	0.02	0.07	0.07	0.49
Indeno[1,2,3-cd]pyrene	-	-	-	-	-	-
Sum:	0.30	0.19	0.34	0.63	0.96	2.90
"Gaseous"	0.23	0.09	0.24	0.33	0.40	1.55
"Aerosol-bound"	0.07	0.10	0.10	0.30	0.56	1.35
Ratio Aeros/Gas (%)	32	112	42	90	141	87

Table A7 GC/MS analysis of sample bags

µg/m^3	east	10m	35m
propene	7.5	8.0	4.4
2-aminopropanol	14.6	15.4	34.5
acetaldehyde	2.5	46.7	22.2
butane	9.6	15.3	19.4
ethanol	42.2	36.6	162.3
pentane	8.8	5.6	8.4
propanol	4.1	1.7	13.8
butanal	6.1	11.3	14.4
2-butanone	14.9	19.6	35.4
hexane	8.1	4.1	6.8
benzene	12.5	7.2	10.6
1-butanol	94.8	18.6	41.1
2-methylpentanal	1.2	1.4	

Table A8 GC/MS analysis of charcoal tubes

µg/m^3	13:00-15:15h			15:30-18:30h		
	east	10m	35m	east	10m	35m
benzene	49.0	70.3	48.5	27.0	75.5	54.0
2,2,3,3 tetramethylbutane	12.2	17.2			23.4	16.2
3-methylhexane	12.4				20.7	15.8
2 propenoicacid,2 methylester	114.3	185.1		39.5	125.4	
methylcyclohexane	24.7					
toluene	95.3	160.9	112.8	69.6	184.3	128.0
2,3,4 trimethylhexane	18.8	27.6	21.7	16.9	27.1	22.0
ethylbenzene	31.8	53.7	41.1	24.5	66.6	42.5
p-xylene	46.9	85.0	66.1	37.1	94.5	58.5
o/m-xylene	24.0	40.2	33.7	15.8	49.9	32.4
1-ethyl,2-methyl benzene	24.4	36.2	50.4	14.4	36.2	20.0
1,2,3 trimethylbenzene	19.3	29.6	25.3	20.6	41.3	21.2
nonanal	31.4	36.5	29.0	37.1	60.5	22.4

Table A9 Results of the analysis of the Sierra HVS stages on heavy metals.

ng/m³ Location	Size (µm)	**Cr**	**Cu**	**Zn**	**Cd**	**Pb**
east	>7	-0.08	0.77	3.00	0.50	1.73
	3-7	0.17	0.44	2.18	0.10	4.79
	1.5-3	0.97	1.50	3.40	0.22	-5.72
	0.95-1.5	-0.08	0.74	3.31	0.18	-1.24
	0.45-0.95	-0.29	0.50	5.65	0.26	-0.82
	<0.45	0.76	7.16	24.09	0.27	-3.96
10m	>7	1.22	4.61	5.44	0.11	5.03
	3-7	0.72	2.65	4.79	0.18	3.66
	1.5-3	0.34	3.00	3.71	0.15	-1.73
	0.95-1.5	0.22	4.64	6.10	0.48	-1.07
	0.45-0.95	0.50	5.29	11.37	0.39	1.24
	<0.45	2.56	10.63	41.79	0.32	23.78
35m	>7	0.30	1.18	1.93	-0.05	-1.42
	3-7	0.87	1.51	2.70	0.00	-2.04
	1.5-3	0.16	1.96	3.06	0.03	-1.17
	0.95-1.5	0.79	2.09	4.46	-0.16	3.66
	0.45-0.95	1.06	1.95	6.93	0.12	6.14
	<0.45	2.04	14.81	37.21	0.70	16.71

Table A10 Meteorogical measurements

Date/Time	Ubar $m.s^{-1}$	Winddir °	T °C	U* $m.s^{-1}$	H $W.m^{-2}$	L m
23-09-98 12:15	3.50	35	13.95	0.233	84	-13.36
23-09-98 12:45	3.38	37	14.05	0.357	189	-21.44
23-09-98 13:00	3.05	22	14.20	0.380	189	-25.84
23-09-98 13:15	2.88	17	14.47	0.362	208	-21.93
23-09-98 13:30	2.69	10	15.17	0.362	207	-24.41
23-09-98 13:45	3.14	29	15.10	0.379	204	-23.69
23-09-98 14:00	3.30	30	15.05	0.422	226	-30.08
23-09-98 14:15	3.57	36	15.01	0.432	209	-34.54
23-09-98 14:30	3.71	40	14.97	0.393	183	-29.88
23-09-98 14:45	3.17	27	15.40	0.396	209	-26.53
23-09-98 15:00	3.23	35	15.42	0.426	201	-34.67
23-09-98 15:15	3.17	33	15.73	0.409	191	-31.91
23-09-98 15:30	3.17	34	16.08	0.386	194	-27.13
23-09-98 15:45	3.23	23	16.35	0.413	161	-39.15
23-09-98 16:00	3.15	23	16.55	0.379	164	-32.40
23-09-98 16:15	3.30	19	16.85	0.457	169	-51.11
23-09-98 16:30	3.45	29	16.75	0.447	157	-51.02
23-09-98 16:45	3.73	34	16.70	0.474	162	-59.05
23-09-98 17:00	3.48	32	17.10	0.454	136	-61.49
23-09-98 17:15	3.70	22	17.07	0.455	105	-82.42
23-09-98 17:30	3.47	25	17.19	0.446	104	-77.83
23-09-98 17:45	3.75	19	17.30	0.469	84	-117.36
23-09-98 18:00	3.45	18	17.24	0.451	68	-123.68
23-09-98 18:15	3.28	14	17.06	0.410	42	-145.27